

# Elastodynamics of Thick Viscous Beams

A. R. Johnson,<sup>1</sup> A. Tessler, and M. Dambach<sup>2</sup>

Computational Structures Branch

NASA Langley Research Center, MS 240

Hampton, VA 23681-0001

15 January 1997

## ABSTRACT

A viscoelastic higher-order thick beam finite element formulation is extended to include elastodynamic deformations. The material constitutive law is a special differential form of the Maxwell solid which employs viscous strains as internal variables to determine the viscous stresses. The total time-dependent stress is the superposition of its elastic and viscous components. In the constitutive model, the elastic strains and the conjugate viscous strains are coupled through a system of first-order ordinary differential equations. The use of the internal strain variables allows for a convenient finite element formulation. The elastodynamic equations of motion are derived from the virtual work principle. Computational examples are carried out for a thick orthotropic cantilevered beam. Relaxation, creep, relaxation followed by free damped vibrations, and damping related modal interactions are discussed.

---

<sup>1</sup> Vehicle Technology Center, Army Research Laboratory.

<sup>2</sup> The George Washington University, Joint Institute for Advancement of Flight Sciences.

## INTRODUCTION

The combination of highly viscous low-modulus matrix materials with high-modulus fibers produces stiff, highly damped load carrying composite structures. The quasi-static and dynamic analyses of such structures require improvements in the material damping representation over the velocity proportional damping schemes. Halpin and Pagano<sup>1</sup> demonstrated that the relaxation moduli for anisotropic solids produce symmetric matrices that can be expanded in a Prony series. Early viscoelastic models for harmonic oscillations of composites computed the complex anisotropic moduli from the elastic properties of the fibers and the complex modulus properties of the matrix material.<sup>2,3</sup> Recently, classical constitutive models have been used for transient deformations including generalized Maxwell and Kelvin-Voigt solids.<sup>4-6</sup> These constitutive models have practical value since they provide adequate approximations for the dynamic softening and hysteresis effects – the phenomena that are not directly proportional to strain rates.

Coleman and Noll,<sup>7</sup> and Schapery<sup>8</sup> presented comprehensive discussions on the history integral form of the viscoelastic constitutive equations. Numerical implementation of the history integral method requires storage of the deformation history. Johnson and co-workers<sup>9-11</sup> developed differential constitutive laws for the large-strain viscoelastic analysis of rubber. The differential formulations do not require that the deformation history be stored. Instead, they require the storage of internal kinematic variables and material property data that requires less memory than the deformation history data. The differential law of Johnson and Stacer<sup>10</sup> was employed in the development of a viscoelastic, large-displacement shell finite element.<sup>12</sup> Recently,

Johnson and Tessler,<sup>13</sup> adopted the same differential constitutive law within Tessler's<sup>14</sup> higher-order beam theory to derive a quasi-static, viscoelastic beam finite element. Their finite element implementation required only minor modifications to an elastic finite element code. The effectiveness and efficiency of the formulation were demonstrated by numerical solutions for the problems of relaxation, creep, and cyclic creep of thick beams.

In this paper, the quasi-static viscoelastic formulation of Johnson and Tessler<sup>13</sup> is extended to elastodynamics. The history integral and differential forms of the constitutive theory for a Maxwell solid are reviewed. The differential form is employed to formulate a viscoelastic higher-order beam finite element. The conditions required for the use of modal methods in the solution of the transient equations are described. The paper concludes with a series of numerical examples which demonstrate the practical and robust aspects of the formulation.

## MAXWELL SOLID IN HISTORY INTEGRAL FORM

Hooke's law for a linearly elastic solid can be written in tensor form as

$$\sigma_{ij} = C_{ijkl} \epsilon_{kl} \quad (1)$$

where  $\sigma_{ij}$ ,  $C_{ijkl}$ , and  $\epsilon_{kl}$  denote respectively the stress, elastic stiffness coefficients or moduli, and strain components. For a linear viscoelastic solid subjected to an instantaneous incremental strain,  $\Delta\epsilon_{kl}$ , the time dependent stress-strain relations take the form

$$\sigma_{ij}(t) = C_{ijkl} \Delta\epsilon_{kl} + \sigma_{ij}^v(t) \quad (2)$$

where the viscous stresses,  $\sigma_{ij}^v(t)$ , decrease monotonically with time. The Boltzmann superposition method is often used to approximate (2) as follows. The viscous stresses are factored such that

$$\sigma_{ij}^v(t) = C_{ijkl}^v(t) \Delta \varepsilon_{kl} \quad (3)$$

The functions  $C_{ijkl}^v(t)$  are referred to as time dependent viscous moduli. These monotonically decreasing functions are approximated in time using a Prony series, i.e.,

$$C_{ijkl}^v(t) = \sum_{n=1}^N C_{ijkl}^n e^{\frac{-t}{\tau_n}} \quad (4)$$

where  $\tau_n \geq 0$ . The stress-strain relations then become

$$\sigma_{ij}(t) = C_{ijkl} \Delta \varepsilon_{kl} + \sum_{n=1}^N C_{ijkl}^n e^{\frac{-t}{\tau_n}} \Delta \varepsilon_{kl} \quad (5)$$

The above approximation is extended to the case of a continuously deforming solid by associating the continuous time dependent strain with an incremental strain history and convoluting (5) in time. The approximation to the time dependent stresses becomes

$$\sigma_{ij}(t) = C_{ijkl} \sum_{m=1}^M \Delta_m \varepsilon_{kl} + \sum_{n=1}^N C_{ijkl}^n \sum_{m=1}^M H(t - t_m) e^{\frac{-(t-t_m)}{\tau_n}} \Delta_m \varepsilon_{kl} \quad (6)$$

where the strain increments at times  $t_m$  are  $\Delta_m \varepsilon_{kl}$  for  $m = 1, \dots, M$ , and use is made of the Heaviside unit step function,  $H(t - t_m)$ . By defining the viscous moduli in terms of the relative time,  $t - t_m$ ,

$$C_{ijkl}^v(t-t_m) = \sum_{n=1}^N C_{ijkl}^n H(t-t_m) e^{\frac{-(t-t_m)}{\tau_n}} \quad (7)$$

the constitutive model in (6) takes the form

$$\sigma_{ij}(t) = C_{ijkl} \sum_{m=1}^M \Delta_m \varepsilon_{kl} + \sum_{m=1}^M C_{ijkl}^v(t-t_m) \Delta_m \varepsilon_{kl} \quad (8)$$

Assuming that strains are smooth functions of time, and taking the limit as  $(t_{m+1} - t_m) \rightarrow 0$  for all  $m$ , gives rise to

$$\sigma_{ij}(t) = C_{ijkl} \varepsilon_{kl}(t) + \int_{\tau=-\infty}^t C_{ijkl}^v(t-\tau) \frac{d\varepsilon_{kl}(\tau)}{d\tau} d\tau \quad (9)$$

where it is noted once again that the viscous moduli,  $C_{ijkl}^v(t-\tau)$ , are monotonically decreasing in time. Equation (9), with the use of (4), is known as the Maxwell solid constitutive model in history integral form.

In many practical applications, adequate time-dependent stress predictions can be obtained with only several terms in the Prony series. However, the numerical approximation of (9) requires that the history of the strain,  $\varepsilon_{kl}(\tau)$ , must be saved which is computationally expensive. Thus, algorithms for (9) must determine the minimum strain history to be retained in order to update the viscous stress approximation accurately as time evolves. When the material can be modeled as a linear Maxwell solid then a recurrence relation can be derived for the finite difference form of (9) and the long term storage of the history is avoided. In what follows we develop an alternative

formulation for (4) and (9) by employing internal variables conjugate to the strain variables allowing (9) to be expressed in full differential form.

#### MAXWELL SOLID IN DIFFERENTIAL FORM

Following Johnson et al.,<sup>9-11</sup> an alternative form of the above constitutive model for a Maxwell solid is derived (also refer to Green and Tobolsky,<sup>15</sup> and to Doi and Edwards<sup>16</sup>). Let us first define a set of internal strain variables,  $\varepsilon_{kl}^n$ , for each time constant in the Prony series, whose increments, at time  $t_m$ , are equal to the increments of the measurable strains. We relax the internal variables between strain increments with the relation

$$\Delta_m \varepsilon_{kl}^n(t - t_m) = H(t - t_m) e^{\frac{-(t-t_m)}{\tau_n}} \Delta_m \varepsilon_{kl} \quad (10)$$

Introducing (10) into (6) results in

$$\sigma_{ij}(t) = C_{ijkl} \sum_{m=1}^M \Delta_m \varepsilon_{kl} + \sum_{n=1}^N C_{ijkl}^n \sum_{m=1}^M \Delta_m \varepsilon_{kl}^n(t - t_m) \quad (11)$$

Assuming the strains are smooth functions of time, and taking the limit as  $(t_{m+1} - t_m) \rightarrow 0$  for all  $m$ , (11) becomes

$$\sigma_{ij}(t) = C_{ijkl} \varepsilon_{kl}(t) + \sum_{n=1}^N C_{ijkl}^n \int_{\tau=-\infty}^t d\varepsilon_{kl}^n(t - \tau) \quad (12)$$

Also, as  $(t_{m+1} - t_m) \rightarrow 0$ , and with  $t_m = \tau$ , (10) becomes

$$d\varepsilon_{kl}^n(t - \tau) = H(t - \tau) e^{\frac{-(t-\tau)}{\tau_n}} d\varepsilon_{kl}(\tau) \quad (13)$$

Integrating (13) with respect to the history,  $\tau$ , yields

$$\varepsilon_{kl}^n(t) = \int_{\tau=-\infty}^t \frac{d\varepsilon_{kl}(\tau)}{d\tau} e^{\frac{-(t-\tau)}{\tau_n}} d\tau \quad (14)$$

Differentiating (14) with respect to the current time,  $t$ , yields

$$\frac{d\varepsilon_{kl}^n(t)}{dt} = -\frac{1}{\tau_n} \left[ \int_{\tau=-\infty}^t \frac{d\varepsilon_{kl}(\tau)}{d\tau} e^{\frac{-(t-\tau)}{\tau_n}} d\tau \right] + \frac{d\varepsilon_{kl}(t)}{dt} \quad (15)$$

Substituting (14) into (15) yields the differential equations for the internal strain variables in the form

$$\frac{d\varepsilon_{kl}^n}{dt} + \frac{\varepsilon_{kl}^n}{\tau_n} = \frac{d\varepsilon_{kl}}{dt} \quad \forall n. \quad (16)$$

Introducing (14) into (12) results in the stress-strain relations given by

$$\sigma_{ij}(t) = C_{ijkl} \varepsilon_{kl}(t) + \sum_{n=1}^N C_{ijkl}^n \varepsilon_{kl}^n(t) \quad (17)$$

Equations (16) and (17) represent the constitutive equations for the Maxwell Solid in differential form. In what follows, these equations are adopted within a higher-order beam theory, and a simple three-node beam element is derived.

## VISCOELASTIC HIGHER-ORDER BEAM

The higher-order beam theory of Tessler<sup>14</sup> coupled with the differential form of the Maxwell solid constitutive equations is discussed in the context of a beam finite element formulation. The beam geometry, kinematics and loading are shown in Figure 1. The

differential form of the viscoelastic constitutive equations consistent with the higher-order beam theory are written in matrix form as

$$\begin{aligned} \mathbf{s}(t) &= \mathbf{C} \mathbf{e} + \sum_{n=1}^N \mathbf{C}^n \mathbf{e}^n(t) \\ \frac{d\mathbf{e}^n}{dt} + \frac{\mathbf{e}^n}{\tau_n} &= \frac{d\mathbf{e}}{dt} \quad \forall n \end{aligned} \quad (18)$$

where  $\mathbf{s}^T = (\sigma_{xx}, \sigma_{zz}, \tau_{xz})$ ,  $\mathbf{e}^T = (\varepsilon_{xx}, \varepsilon_{zz}, \gamma_{xz})$ ,  $\mathbf{e}^{nT} = (\varepsilon_{xx}^n, \varepsilon_{zz}^n, \gamma_{xz}^n)$

$$\mathbf{C} = \begin{bmatrix} C_{11} & C_{13} & 0 \\ C_{13} & C_{33} & 0 \\ 0 & 0 & C_{55} \end{bmatrix} \text{ and } \mathbf{C}^n = \begin{bmatrix} C_{11}^n & C_{13}^n & 0 \\ C_{13}^n & C_{33}^n & 0 \\ 0 & 0 & C_{55}^n \end{bmatrix}$$

The vectors  $\mathbf{s}$  and  $\mathbf{e}$  are the engineering stresses and strains. The vectors  $\mathbf{e}^n$  ( $n = 1, 2, \dots, N$ ) are the internal variables, i.e., conjugate viscous strains, where  $N$  is the number of terms in a Prony series representation of the material's stress relaxation response. The matrices  $\mathbf{C}$  and  $\mathbf{C}^n$  contain the elastic and viscous moduli. In the higher-order beam theory,<sup>14</sup> the components of the displacement vector are approximated through the beam thickness by way of five kinematic variables, i.e.,

$$\begin{aligned} u_x(x, z, t) &= u(x, t) + h\zeta\theta(x, t) \\ u_z(x, z, t) &= w(x, t) + \zeta w_1(x, t) + \left(\zeta^2 - \frac{1}{5}\right)w_2(x, t) \end{aligned} \quad (19)$$

where  $\zeta = z/h$  denotes a nondimensional thickness coordinate and  $2h$  is the total thickness. The function  $u(x, t)$  represents the midplane (i.e. reference plane) axial displacement,  $\theta(x, t)$  is the bending rotation of the cross-section of the beam,  $w(x, t)$  is a weighted-average transverse deflection, and  $w_1(x, t)$  and  $w_2(x, t)$  are the higher-order



transverse displacement variables enabling a parabolic distribution of  $u_z(x, z, t)$  through the thickness. In addition to the displacement assumptions, (19), this beam theory employs independent assumptions upon the  $\varepsilon_{zz}$  and  $\gamma_{xz}$  that are respectively cubic and quadratic through the beam thickness.

The above displacement and strain assumptions give rise to axial, transverse normal and transverse shear strains of the form

$$\begin{aligned}\varepsilon_{xx} &= u(x, t)_{,x} + h\zeta\theta(x, t)_{,x} \\ \varepsilon_{zz} &= \frac{w_1(x, t)}{h} + \phi_z(\zeta) \frac{w_2(x, t)}{h^2} + \phi_x(\zeta) \theta(x, t)_{,x} \\ \gamma_{xz} &= \phi_{xz}(\zeta) (w(x, t)_{,x} + \theta(x, t))\end{aligned}\tag{20}$$

where  $\phi_x(\zeta) = h\nu_{13}\zeta(4 - 7\zeta^2)/17$ ,  $\phi_z(\zeta) = 14\zeta h(3 - \zeta^2)/17$ ,

$\phi_{xz}(\zeta) = 5(1 - \zeta^2)/4$ , and  $\nu_{13}$  is Poisson's ratio. The simplest finite element

approximation of this beam theory involves a three-node configuration (see Figure 2)

which is achieved by the following interpolations

$$\begin{aligned}u(\eta, t) &= (1 - \eta)u_0^\ell(t) + \eta u_1^\ell(t), \quad \theta(\eta, t) = (1 - \eta)\theta_0^\ell(t) + \eta\theta_1^\ell(t), \\ w(\eta, t) &= (1 - \eta)w_0^\ell(t) + \eta w_1^\ell(t) - \frac{\ell}{2}\eta(1 - \eta)(\theta_0^\ell(t) - \theta_1^\ell(t)), \\ w_1(\eta, t) &= W_1^\ell(t), \quad w_2(\eta, t) = W_2^\ell(t)\end{aligned}\tag{21}$$

where  $\eta = x/\ell$  is the nondimensional axial coordinate. The nodal degrees-of-freedom at the two ends of the element have subscripts 0 and 1 respectively. Since the strains do not possess derivatives of the  $w_1(\eta, t)$  and  $w_2(\eta, t)$  variables, these variables need not be

continuous at the element nodes and, hence, their simplest approximation is constant for each element. Their corresponding degrees-of-freedom are attributed to a node at the element midspan.

For dynamic loading, the virtual work statement for an element of volume  $V$  with the differential Maxwell constitutive law can be written as

$$\begin{aligned} & \int \rho \left( \frac{d^2 u_x}{dt^2} \delta u_x + \frac{d^2 u_z}{dt^2} \delta u_z \right) dV + \int \mathbf{e}^T \mathbf{C} \delta \mathbf{e} dV \\ & + \sum_{n=1}^N \int \mathbf{e}^{nT} \mathbf{C}^n \delta \mathbf{e}^n dV - \delta W = 0 \end{aligned} \quad (22)$$

where the first integral represents the virtual work done by inertial forces, the second is the internal virtual work done by the elastic stresses, the third is the internal virtual work done by the viscous stresses, and  $\delta W$  is the virtual work done by the external forces. Introducing (21) into (19) and substituting the results into (20) yields finite element approximations of the strains in terms of the nodal variables, i.e.,

$$\mathbf{e} = \mathbf{B} \mathbf{u}, \quad (23)$$

$$\mathbf{B} = \begin{bmatrix} -\frac{1}{\ell} & 0 & -\frac{z}{\ell} & 0 & 0 & \frac{1}{\ell} & 0 & \frac{z}{\ell} \\ 0 & 0 & -\frac{\phi_x}{\ell} & \frac{1}{h} & \frac{\phi_z}{h^2} & 0 & 0 & \frac{\phi_x}{\ell} \\ 0 & -\frac{\phi_{xz}}{\ell} & \frac{\phi_{xz}}{2} & 0 & 0 & 0 & \frac{\phi_{xz}}{\ell} & \frac{\phi_{xz}}{2} \end{bmatrix}$$

and  $\mathbf{u}^T = (u_0, w_0, \theta_0, W_1, W_2, u_1, w_1, \theta_1)$  denotes the element nodal displacement vector. Next, a set of analogous nodal variables,  $\mathbf{u}^n$ , and corresponding viscous strains,  $\mathbf{e}^n$ , are introduced. These are related by

$$\mathbf{e}^n = \mathbf{B} \mathbf{u}^n \quad (24)$$

The  $\mathbf{u}^n$  variables, which carry the time dependent information for the material within the element, are independent from element to element. The displacements  $u_x$  and  $u_z$  are then expressed in terms of the element nodal degrees-of-freedom using (19) and (21), giving rise to  $u_x = \Phi_x^T \mathbf{u}$  and  $u_z = \Phi_z^T \mathbf{u}$ , where  $\Phi_x(\zeta, \eta)$  and  $\Phi_z(\zeta, \eta)$  are vectors of the interpolation functions. The virtual work statement for an element then becomes

$$\begin{aligned} & \frac{d^2 \mathbf{u}^T}{dt^2} \int \rho (\Phi_x \Phi_x^T + \Phi_z \Phi_z^T) dV \delta \mathbf{u} + \mathbf{u}^T \int \mathbf{B}^T \mathbf{C} \mathbf{B} dV \delta \mathbf{u} \\ & + \sum_{n=1}^N \mathbf{u}^{nT} \int \mathbf{B}^T \mathbf{C}^n \mathbf{B} dV \delta \mathbf{u}^n - \delta W = 0 \end{aligned} \quad (25)$$

By defining the integrals in (25) as the mass,  $\mathbf{m}$ , elastic stiffness,  $\mathbf{k}$ , and viscous stiffness,  $\mathbf{k}^n$ , matrices, there results

$$\left[ \frac{d^2 \mathbf{u}^T}{dt^2} \mathbf{m} + \mathbf{u}^T \mathbf{k} \right] \delta \mathbf{u} + \left[ \sum_{n=1}^N \mathbf{u}^{nT} \mathbf{k}^n \delta \mathbf{u}^n \right] - \delta W = 0 \quad (26)$$

Since  $\delta \mathbf{u} = \delta \mathbf{u}^n$  when  $t$  is constant, the virtual work takes on a simpler form

$$\left[ \frac{d^2 \mathbf{u}^T}{dt^2} \mathbf{m} + \mathbf{u}^T \mathbf{k} + \sum_{n=1}^N \mathbf{u}^{nT} \mathbf{k}^n \right] \delta \mathbf{u} - \delta W = 0 \quad (27)$$

This implies that at any time  $t$  the element equilibrium equations are

$$\mathbf{m} \frac{d^2 \mathbf{u}}{dt^2} + \mathbf{k} \mathbf{u} = \mathbf{f} - \sum_{n=1}^N \mathbf{k}^n \mathbf{u}^n \quad \text{for each element} \quad (28)$$

where  $\mathbf{f}$  denotes the element consistent load vector due to the external loading. Introducing (23) and (24) into the differential equations for the strain variables in (18) yields

$$\frac{d\mathbf{u}^n}{dt} + \frac{\mathbf{u}^n}{\tau_n} = \frac{d\mathbf{u}}{dt} \quad \forall n. \quad (29)$$

The global equilibrium equations are determined by the standard assembly of the element equations, (28), and there is no assembly for (29). The global equations of motion can be written as

$$\mathbf{M} \frac{d^2 \mathbf{u}_g}{dt^2} + \mathbf{K} \mathbf{u}_g = \mathbf{F}_{mech} - \mathbf{F}_{visc} \quad (30)$$

where  $\mathbf{u}_g$  denotes the global nodal variable vector,  $\mathbf{M}$  is the mass matrix,  $\mathbf{K}$  is the elastic stiffness matrix,  $\mathbf{F}_{mech}$  is the global force vector due to mechanical loads, and  $\mathbf{F}_{visc}$  is the assembled vector for  $\sum_{n=1}^N \mathbf{k}^n \mathbf{u}^n$ . The viscoelastic problem is solved by

simultaneously integrating the first order differential equations, (29), and the second order equations, (30), where the latter is subject to the appropriate boundary restraints.

As far as the finite element implementation is concerned, a conventional linear elastic code can be readily adapted to perform a dynamic analysis for a structure made from a Maxwell material. The viscous stiffness coefficients,  $C_{ij}^n$ , are used to compute the element viscous stiffness matrices,  $\mathbf{k}^n$ , which are stored for repeated use. The internal nodal variables for each element,  $\mathbf{u}^n$ , are set equal to their initial values. An iterative Newmark algorithm is then used to integrate (29) and (30). The modification of

Newmark's algorithm is required so that (29), the internal variable evolution equations, are implicitly integrated with the trapezoidal method.

## CONDITIONS FOR MODAL ANALYSIS

When a Voight solid is used to determine the damping forces (i.e.,  $\mathbf{F}_{visc} = \mathbf{C}_d \frac{d\mathbf{u}_g}{dt}$ ) the damping matrix,  $\mathbf{C}_d$ , is often assumed to be proportional to  $\mathbf{M}$  and/or to  $\mathbf{K}$  so that the transient motion can be studied using modal methods. For the Maxwell solid presented above, when the element viscous stiffness matrices,  $\mathbf{k}^n$ , are proportional to the element's elastic stiffness matrix (i.e.,  $\mathbf{k}^n = \alpha_n \mathbf{k}$ ,  $\alpha_n = \text{constants}$ ) and when the time constants,  $\tau_n$ , are the same for all elements, the global equations of motion can be studied using modal methods. This is accomplished as follows. First, the mode shapes,  $\mathbf{e}_i$ , and frequencies,  $\omega_i$ , are determined by solving

$$(\mathbf{K} - \omega_i^2 \mathbf{M}) \mathbf{e}_i = \mathbf{0} \quad (31)$$

where the modal vectors are normalized with respect to the mass matrix so that  $\mathbf{e}_i^T \mathbf{M} \mathbf{e}_j = \delta_{ij}$ . In analogy with the case of a Voight solid, the condition for uncoupling the homogenous form of (29) and (30) is determined. Under the above assumptions of material behavior it can be shown that the global viscous nodal forces are related to global viscous displacement vectors by

$$\mathbf{F}_{visc} = \sum_n \mathbf{K}^n \mathbf{u}_g^n = \mathbf{K} \sum_n \alpha_n \mathbf{u}_g^n \quad \text{and}$$

$$\frac{d\mathbf{u}_g^n}{dt} + \frac{\mathbf{u}_g^n}{\tau_n} = \frac{d\mathbf{u}_g}{dt} \quad \forall n. \quad (32)$$

Using the mode shapes, the transient motion can be expressed as

$$\mathbf{u}_g(t) = \sum_i c_i(t) \mathbf{e}_i \quad \text{and} \quad \mathbf{u}_g^n(t) = \sum_i b_i^n(t) \mathbf{e}_i \quad (33)$$

With (33) the homogenous form of (29) and (30) becomes

$$\sum_i \left( \frac{d^2 c_i}{dt^2} \mathbf{M} + \left( c_i + \sum_n \alpha_n b_i^n \right) \mathbf{K} \right) \mathbf{e}_i = \mathbf{0}$$

$$\sum_i \left( \frac{db_i^n}{dt} + \frac{b_i^n}{\tau_n} - \frac{dc_i}{dt} \right) \mathbf{e}_i = \mathbf{0} \quad \forall n \quad (34)$$

Premultiplying (34) by  $\mathbf{e}_j^T$  and  $\mathbf{e}_j^T \mathbf{M}$  respectively results in

$$\frac{d^2 c_j}{dt^2} + \omega_j^2 \left( c_j + \sum_n \alpha_n b_j^n \right) = 0$$

$$\frac{db_j^n}{dt} + \frac{b_j^n}{\tau_n} - \frac{dc_j}{dt} = 0 \quad \forall n \quad (35)$$

Equations (35) represent a system of uncoupled first and second order ordinary differential equations for the modal functions  $b_j^n(t)$  ( $n = 1, 2, \dots$ ) and  $c_j(t)$ . In general, the element viscous stiffness matrices,  $\mathbf{k}^n$ , are not expected to be proportional to the element elastic stiffness matrix,  $\mathbf{k}$ , in each element. For example, the stiffness matrices  $\mathbf{k}^n$  for a composite are expected to be highly dependent on the matrix material which has isotropic properties. In contrast, the elastic stiffness matrix,  $\mathbf{k}$ , depends on the

anisotropic properties of the fibers. Consequently, the dynamic response of a composite structure is expected to possess a certain degree of modal coupling, depending on the respective magnitudes of the elastic and viscous moduli.

## APPLICATIONS

Numerical solutions representative of quasi-static and free vibration deformations of a thick cantilevered orthotropic beam are presented. The beam shown in Figure 1 has the following dimensions:  $L = 0.2\text{m}$ ,  $2h = 0.02\text{m}$ , and  $b = 1.0\text{m}$ . The plane-stress elastic moduli can be expressed in terms of engineering material constants as

$$C_{11} = E_x / (1 - \nu_{xz} \nu_{zx}), \quad C_{33} = E_z / (1 - \nu_{xz} \nu_{zx}), \quad C_{13} = \nu_{xz} C_{33}, \quad C_{55} = G_{xz}$$

A unidirectional E-glass/epoxy laminate is considered<sup>17</sup> for which the material constants are:  $E_x = 38.6\text{GPa}$ ,  $E_z = 8.27\text{GPa}$ ,  $G_{xz} = 4.14\text{GPa}$ ,  $\nu_{xz} = 0.26$ , and  $\rho = 1.8\text{g/cm}^3$ . To demonstrate relaxation, creep, and high frequency damped vibration, the viscous matrices  $\mathbf{C}^n$  are assumed proportional to the elastic matrix  $\mathbf{C}$  as follows:

$$\mathbf{C}^1 = \mathbf{C}^2 = \frac{1}{10} \mathbf{C}. \quad \text{The relaxation times are } \tau_1 = 0.1 \text{ and } \tau_2 = 0.001. \text{ Thus, the}$$

time dependent constitutive matrix is

$$\mathbf{C}(t) = \mathbf{C} \left[ 1.0 + \frac{1}{10} e^{-0.1t} + \frac{1}{10} e^{-0.001t} \right]$$

The beam is uniformly discretized with 32 elements for the relaxation, creep, and relaxation-free vibration problems, whereas the modal interaction example employed a 50 element model.

Relaxation: A cantilever beam (Figure 1) with  $w, u, \theta$  fixed at point A has a prescribed deflection  $w$  at point B that is ramped from 0 to -0.0319m in 0.05 sec and then held constant. Figure 3 depicts the maximum axial stress at the top surface of the clamped end (point C) as a function of time. Also shown are the elastic and viscous stress components which comprise the total stress. The decay of the total viscoelastic stress to its elastic value as time is increased demonstrates the expected step-strain relaxation behavior.

Creep: In this example, the cantilevered beam has a prescribed concentrated vertical force applied at point B that is ramped from 0 to -300 kN in 0.05 sec and then held constant. Figure 4 depicts the tip deflection as a function of time. The creep response of the beam is shown along with its elastic response to the same loading. Figure 5 shows the time-dependent transverse shear strain through the thickness at the clamped end.

Relaxation-Free Vibration: This example demonstrates the the capability of the present constitutive law to simulate a material response over a wide range of strain rates. Following the Relaxation example above, the tip of the beam (the location of the prescribed displacement) is released at  $t = 0.1$  sec. Figure 6 depicts the high frequency damped axial stress at point C as a function of time.

Modal Interaction: Modal interaction due to material damping is investigated using two distinct material models. The first model, referred to as the proportional model, is the one described above. It meets the requirements for modal analysis. The second model represents the case in which the viscous matrices  $\mathbf{C}^n$  are not proportional to the elastic matrix  $\mathbf{C}$ . Instead, the damping is isotropic with material constants:



$E_x = E_z = 3.86\text{GPa}$ ,  $G_{xz} = 0.414\text{GPa}$ , and  $\nu_{xz} = \nu_{zx} = 0.35$ . A discretization study of the elastic vibration modes, (31), determines that a uniform mesh with 32 elements can adequately approximate the first thirteen modes. Mode thirteen is a bending mode with a half wavelength approximately equal to the thickness of the beam and represents the limit of validity of the higher-order beam theory. Free damped vibration transient analyses were then performed, using 50 elements. The initial shape of the beam was mode 7 (also a bending mode) and the initial velocity was zero. The transient analysis for this proportional model showed no modal interaction. That is, the contribution of the kinetic energy in modes other than mode 7 were double precision zeros relative to the mode 7 value at each time step. Mode 7 damped out without exciting other modes. In the case of the nonproportional model, more than 99.0% of the kinetic energy is attributed to mode 7; however, mode 3 (a bending mode) is also excited and contributed to about 0.5% of the kinetic energy with the other modes contributing smaller amounts.

## CONCLUSION

An elastodynamic formulation, which includes a differential form of the Maxwell viscous solid constitutive theory, has been implemented in a higher-order-theory beam finite element. The attractive features of the formulation include: (a) The use of constitutive constants that are the same as those of the classical history-integral model. These constants are readily available from step-strain relaxation tests, (b) The internal variables are conjugate to the elastic strain measures; hence, they are consistent with the

kinematic assumptions of the elastic formulation, (c) The update of the internal variables can be performed in a parallel computing environment, allowing the viscous force vector in the equations of motion to be determined efficiently within the modified Newmark algorithm, (d) Applications of time-dependent displacements and loads are performed within the same finite element algorithm, and (f) The higher-order beam theory accounts for both transverse shear and transverse normal deformations — the effects that need to be accounted for in thick and highly orthotropic beams, and in high-frequency dynamics.

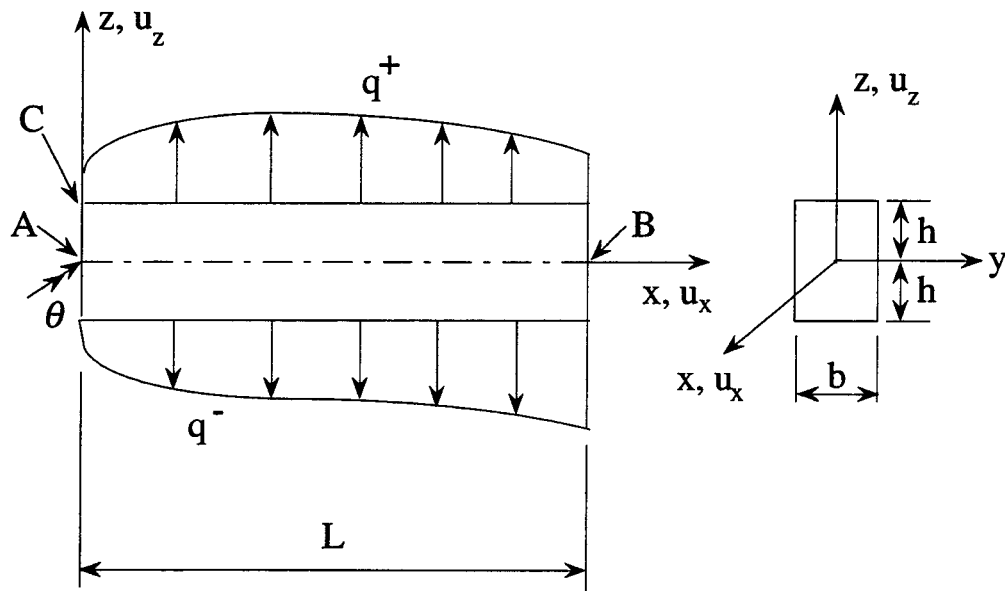
The numerical examples clearly demonstrate the capability of this finite element formulation to simulate physically important phenomena that are computationally difficult to obtain by other approaches.

## REFERENCES

1. Halpin, J. C., and Pagano, N. J., Observations on linear anisotropic viscoelasticity, *J. Composite Materials*, **2**, No. 1, 68-80 (1968).
2. Hashin, Z., Complex moduli of viscoelastic composites - I. General theory and applications to particulate composites, *Int. J. Solids Structures*, **6**, 539-552 (1970).
3. Hashin, Z., Complex moduli of viscoelastic composites - II. Fiber reinforced materials, *Int. J. Solids and Structures*, **6**, 797-807 (1970).
4. Argyris, J., St. Doltsinis, I., and daSilva, V. D., Constitutive modeling and computation of non-linear viscoelastic solids, Part I. Rheological models and numerical integration techniques, *Comput. Methods Appl. Mech. Engrg.*, **88**, 135-163 (1991).

5. Shaw, S., Warby, M. K., and Whiteman, J. R., Numerical techniques for problems of quasistatic and dynamic viscoelasticity, J. R. Whiteman (editor), in The Mathematics of Finite Elements and Applications, Highlights 1993, 45-68, John Wiley & Sons (1994).
6. Shaw, S. and Whiteman, J. R., Towards robust adaptive finite element methods for partial differential Volterra equation problems arising in viscoelasticity, J. R. Whiteman (editor), The Mathematics of Finite elements and Applications, Highlights 1996, 55-80, John Wiley, Chichester, 1997.
7. Coleman, B. D., and Noll, W., Foundations of linear viscoelasticity, *Reviews of Modern Physics*, **33**, No.2, 239-249 (1961).
8. Schapery, R. A., Viscoelastic behavior and analysis of composite materials, in Composite Materials, **2**, edited by G. P. Sendeckyj, Academic Press (1974).
9. Johnson, A. R. and Quigley, C. J., A viscohyperelastic Maxwell model for rubber viscoelasticity, *Rubber Chemistry and Technology*, **65**, No.1, 137-153 (1992).
10. Johnson, A. R., and Stacer, R. G., Rubber viscoelasticity using the physically constrained system's stretches as internal variables, *Rubber Chemistry and Technology*, **66**, No.4, 567-577 (1993).
11. Johnson, A. R., Quigley, C. J., and Freese, C. E., A viscohyperelastic finite element model for rubber, *Comput. Meths. Appl. Mech. Engrg.*, **127**, 163-180 (1995).
12. Johnson, A. R., Tanner, J. A., and Mason, A. J., A kinematically driven anisotropic viscoelastic constitutive model applied to tires, in Computational Modeling of Tires, compiled by A. K. Noor and J. A. Tanner, NASA Conference Publication 3306, August 1995.

13. Johnson, A. R., and Tessler, A., A viscoelastic higher-order beam finite element, NASA TM 110260, June 1996; also in J. R. Whiteman (editor), The Mathematics of Finite elements and Applications, Highlights 1996, 333 - 345, John Wiley, Chichester, 1997.
14. Tessler, A., A two-node beam element including transverse shear and transverse normal deformations, Int. J. for Numer. Methods Eng., **32**, 1027-1039 (1991).
15. Green, M. S., and Tobolsky, A. V., A new approach to the theory of relaxing polymeric media, J. Chem. Phys., **14**(2), 80-92 (1946).
16. Doi, M., and Edwards, S. F., The Theory of Polymer Dynamics, Oxford, New York, 1986.
17. Tsai, S. W., Massard, T. N., and Susuki, I., Composites Design - 1985, Think Composites, Dayton, OH (1985).



Clamped conditions applied at point A.

Enforced displacements and concentrated loads applied at point B.

Surface stress  $\sigma_{xx}$  computed at point C.

Figure 1. Beam geometry, kinematics, and loading.

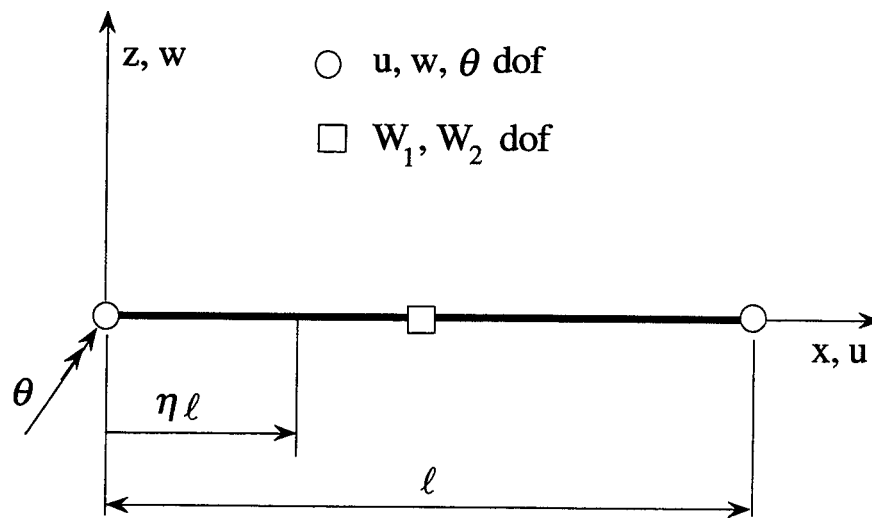


Figure 2. A three-node, higher-order-theory beam element.

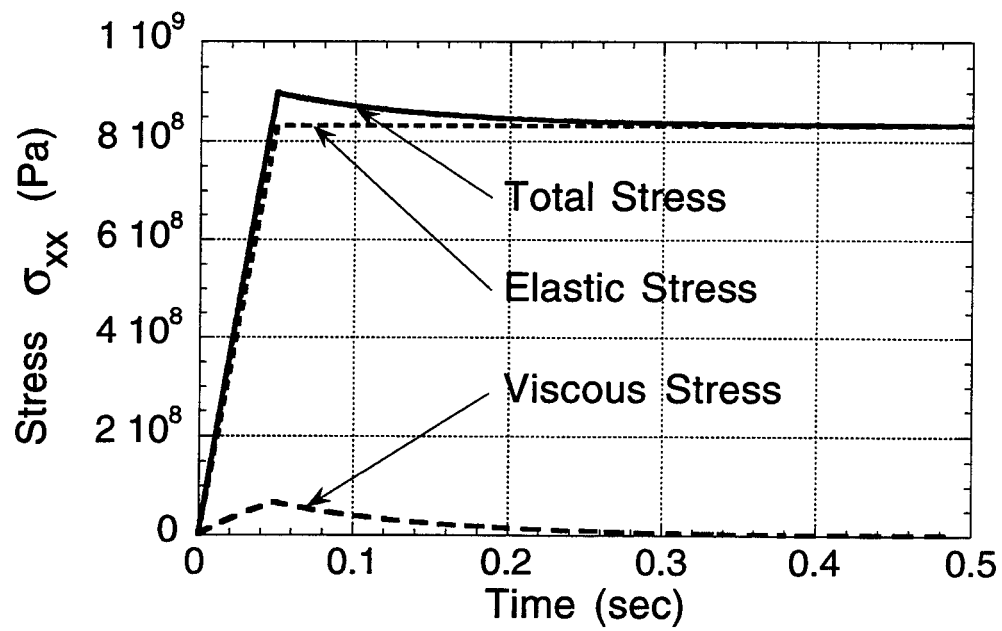


Figure 3. Cantilevered beam under prescribed tip deflection. Stress on top surface of clamped end (point C).

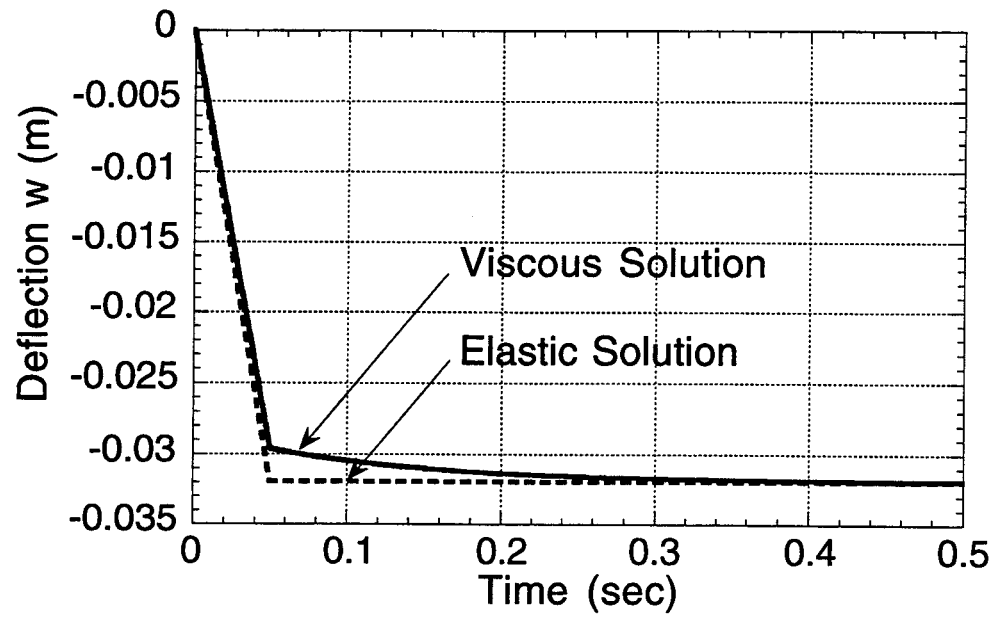


Figure 4. Cantilevered beam under prescribed tip load. Tip deflection.



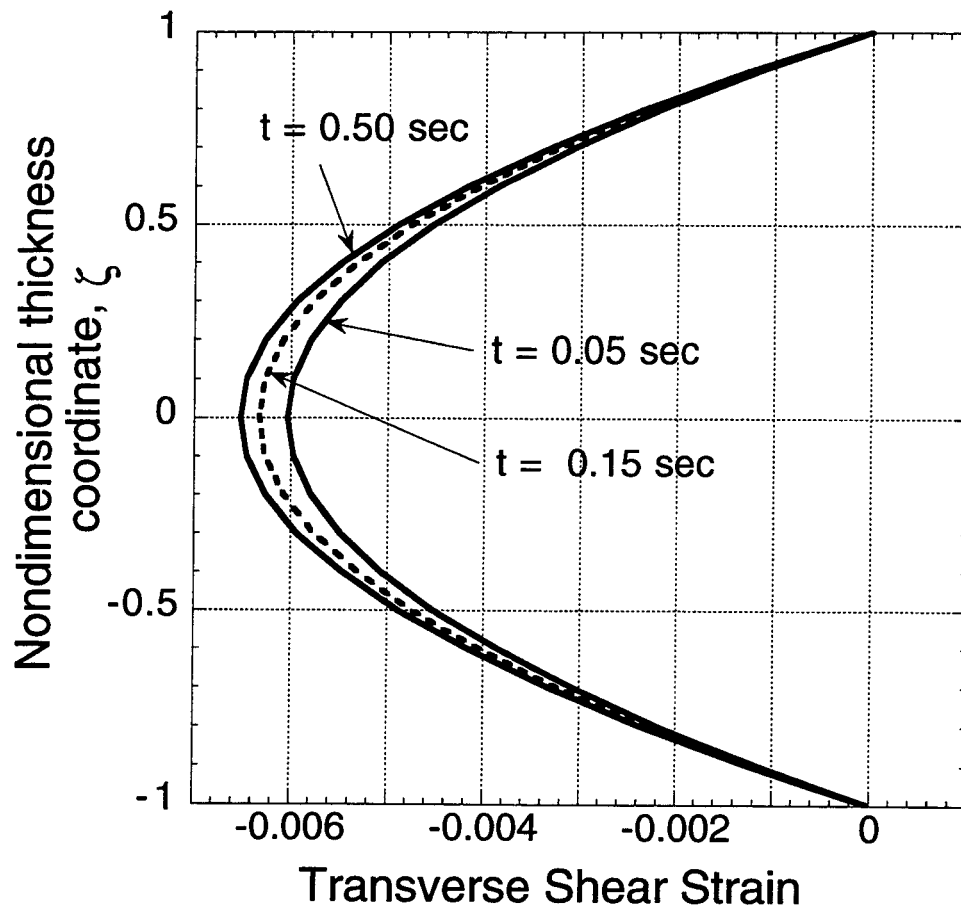


Figure 5. Cantilevered beam under prescribed tip load. Transverse shear strain at support.

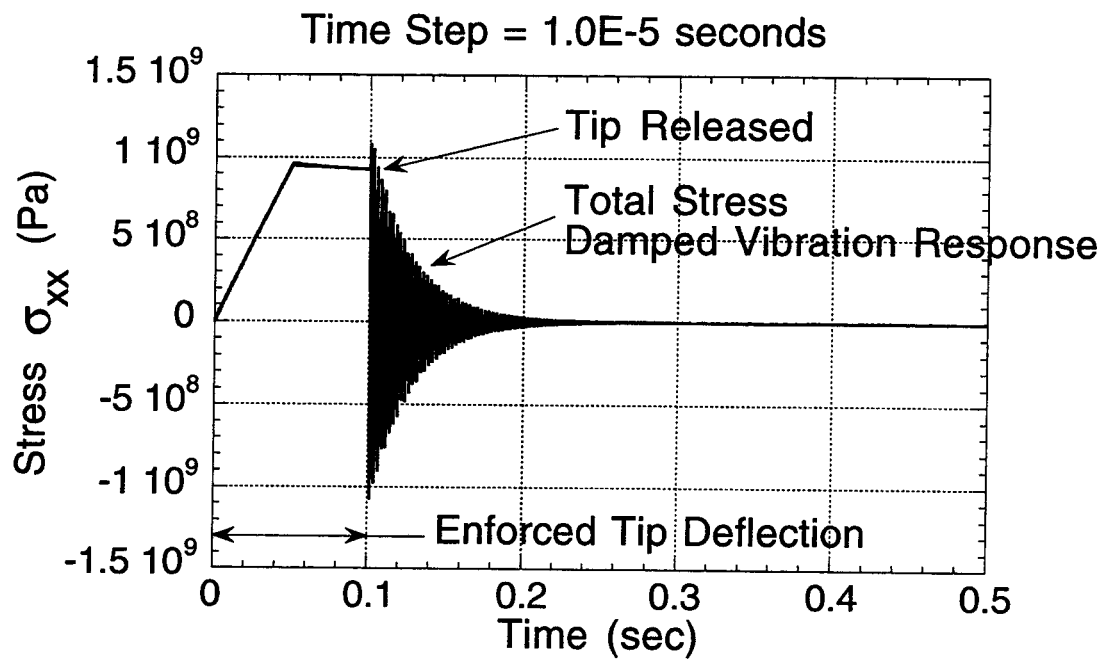


Figure 6. Cantilevered beam under prescribed tip deflection and tip released. Stress on top surface at clamped end.